The effects of tilt on interferometric rotation sensors

D.N. Pham, H. Igel , J. Wassermann, A. Cochard, U. Schreiber

Corresponding Author:

Heiner Igel

Geophysics Section, Department of Earth and Environmental Sciences, LMU Munich,

Theresienstr. 41, 80333 Munich, GERMANY.

Phone: +49 (89) 2180-4204

Fax: +49 (89) 2180-4205

Email: heiner.igel@geophysik.uni-muenchen.de

Abstract

Ring laser rotation sensors are contaminated by rotations around horizontal axes (also called tilts) through the vector product between the local normal direction and the vector of the rotation rate composed of Earth's rotation and local ground rotations. In this study, we investigate theoretically this cross-axis sensitivity and estimate the effects based on magnitude-amplitude relations to be expected for observations of local earthquakes and tele-seismic events. We investigate tilt-ring laser coupling for rotational motions in the P coda of several past earthquakes using tilt motions derived from observed translations. The results show that compared to the corresponding vertical rotation rate tilt-ring laser coupling is negligible for observations of tele-seismic events and for the applicable range of the local magnitude scale.

Introduction

With ring laser technology seismologists can now observe rotational ground motions for a wide magnitude and distance range (Pancha et al. 2000; Schreiber et al. 2005, 2006; Igel et al. 2005, 2007). Amplitudes of ring laser rotational signals are used to estimate of phase velocities (Igel et al. 2007), or constrain subsurface properties (Pham et al. 2008; Fichtner and Igel, 2008). Moreover, amplitude and waveform modelling of rotational motions requires quantitative understanding of all factors contributing to the signals. Therefore, each effect that contributes to ring laser measurements has to be considered carefully.

Although ring laser rotation sensors are built to be insensitive to translations, their records are contaminated by horizontal components of rotations or co-seismic tilts (McLeod et al. 1998; Schreiber et al. 2005, 2006, 2008). Tilt-ring laser coupling therefore may potentially contribute to ring-laser measurements. However, this effect was so far not looked at in a quantitative way or in connection with observed rotations. In addition, previous rough estimates of tilt-ring laser coupling were erroneously based on tiltmeter measurements that are primarily sensitive to horizontal acceleration in the frequency band considered.

The main goal of this study is to investigate quantitatively the effects of co-seismic tilts on ring laser measurements. While the problem in itself deserves attention, the main motivation for the present study comes from observation of rotational motions

in the P coda (Igel et al. 2007; Pham et al. 2008). In order to understand the origin of these signals all potential contributions need to be quantified. In the present study the focus is on tilt-ring laser coupling in general with specific applications to local and tele-seismic events. The tilt-ring laser coupling is evaluated based on the comparison with the corresponding vertical rotation rate. Thus, the so-called significant (or negligible) tilt-ring laser coupling in this study means the tilt-ring laser coupling to be significant (or negligible) compared to the corresponding vertical rotation rate.

We first investigate theoretically tilt-ring laser coupling and perform estimates of the effects based on magnitude-amplitude relations to be expected for observations of local earthquakes and tele-seismic events. We then apply the theory to the observations in the P coda. We estimate tilt-ring laser coupling in the P coda of several observed events based on translation derived tilts (Li et al. 2001). We conclude that the effects can be neglected for observations of tele-seismic events and for the applicable range of the local magnitude scale.

Tilt - ring laser coupling: theory

Ring laser sensors allow us to observe rotational ground motions with high accuracy through the Sagnac effect (Schreiber et al. 2005, 2006; Igel et al. 2007):

$$\Delta f = \frac{4A}{\lambda P}\mathbf{n}_R \bullet \dot{\mathbf{\Omega}} \qquad (1)$$

where A, P, and $\mathbf{n}_R$, respectively, are area, perimeter and normal unit vector of the ring laser, $\dot{\mathbf{\Omega}}$ is the vector of the imposed rotation rate, λ is laser wavelength, Δf is the Sagnac frequency.

Equation (1) is called the Sagnac equation demonstrating that there are three contributions that influence the Sagnac frequency Δf: 1) changes of the scale factor $\frac{4A}{\lambda P}$ under the effects of seismic deformation, temperature variation of the medium etc. Since the mechanical instrument was extremely rigid and stable, the effects of the scale factor can be avoided (Schreiber et al. 2006); 2) variations in $\dot{\mathbf{\Omega}}$ itself; 3) changes in orientation of $\mathbf{n}_R$ when the sensor is tilted by seismic waves and as a result of the inner product, it changes the Sagnac frequency (McLeod et al. 1998; Schreiber et al. 2006). This phenomenon – called "tilt – ring laser coupling" or shortly "tilt coupling" or "tilt effects" - will be investigated in the following as it is a potential cause for ring-laser signals in the P coda reported by Igel et al. (2007) and Pham et al. (2008).

To quantify the tilt - ring laser coupling, we look at equation (1) in detail. As mentioned by McLeod et al. (1998), $\dot{\mathbf{\Omega}}$ contains both contributions of the Earth's rotation rate and the seismically induced rotation rate. On the surface of the Earth, the seismically induced rotation rate can be expressed by three orthogonal components (vertical, N-S and E-W). Thus, (1) can be re-written by:

$$\Delta f = \frac{4A}{\lambda P}\mathbf{n}_R \bullet (\dot{\Omega}_P \mathbf{n}_P + \dot{\Omega}_Z \mathbf{n}_Z + \dot{\Omega}_N \mathbf{n}_N + \dot{\Omega}_E \mathbf{n}_E) \qquad (2)$$

$\dot{\Omega}_P$: Rotation rate of the Earth around its rotation axis.

$\dot{\Omega}_Z$, $\dot{\Omega}_N$, $\dot{\Omega}_E$: Seismically induced rotation rates around vertical, NS and EW axes, respectively.

$\mathbf{n}_P$, $\mathbf{n}_Z$, $\mathbf{n}_N$, and $\mathbf{n}_E$: The unit basis vectors of the rotation axis of the Earth, vertical, NS, and EW axes, respectively.

Expanding the inner product in (2) we have:

$$\Delta f = \frac{4A}{\lambda P}\left[\dot{\Omega}_P \alpha_P + \dot{\Omega}_Z \alpha_Z + \dot{\Omega}_N \alpha_N + \dot{\Omega}_E \alpha_E\right] \qquad (3)$$

Here α_P, α_Z, α_N, and α_E are cosines of the angles between $\mathbf{n}_R$ and $\mathbf{n}_P$, $\mathbf{n}_Z$, $\mathbf{n}_N$, $\mathbf{n}_E$ (respectively) that can be calculated as the functions of the EW and NS horizontal components of seismically induced rotations Ω_E, Ω_N (or co-seismic tilts) and the latitude of the ring laser location Λ (see Appendix A1).

Equation (3) contains the cross-axis sensitivity of a ring laser. In case $\Omega_E = 0$ and $\Omega_N = 0$ (there is no tilt), we will have $\alpha_P = \sin(\Lambda), \alpha_Z = 1$, $\alpha_N = \alpha_E = 0$, and equation (3) simplifies to:

$$\Delta f = \frac{4A}{\lambda P}\left[\dot{\Omega}_P \sin(\Lambda) + \dot{\Omega}_Z\right] \tag{4}$$

In several past studies (e.g. Suryanto et al. 2006, Igel et al. 2005, 2007) the co-seismic tilts Ω_E, Ω_N are assumed negligible for tele-seismic events, thus the observed vertical rotation rates was extracted from the Sagnac frequency according to equation (4). In general, as indicated by equation (3), such inferred rotation rate includes the contribution of tilt coupling. Thus, here we call it the contaminated rotation rate $\dot{\Omega}_{Z(cont.)}$ defined as:

$$\dot{\Omega}_{Z(cont.)} = \Delta f \frac{\lambda P}{4A} - \dot{\Omega}_P \sin(\Lambda) \tag{5}$$

Combining (5) and (3) leads to:

$$\dot{\Omega}_{Z(cont.)} = \dot{\Omega}_P\left[\alpha_P - \sin(\Lambda)\right] + \dot{\Omega}_Z\alpha_Z + \dot{\Omega}_N\alpha_N + \dot{\Omega}_E\alpha_E \tag{6}$$

In our subsequent calculations, we define tilt – ring laser coupling $\dot{\Omega}_{Tilt}$ as the difference between the contaminated rotation rate $\dot{\Omega}_{Z(cont.)}$ and purely seismically-induced rotation rate $\dot{\Omega}_Z$:

$$\dot{\Omega}_{Tilt} = \dot{\Omega}_{Z(cont.)} - \dot{\Omega}_Z$$

$$\dot{\Omega}_{Tilt} = \dot{\Omega}_P\left[\alpha_P - \sin(\Lambda)\right] + \dot{\Omega}_Z\left(\alpha_Z - 1\right) + \dot{\Omega}_N\alpha_N + \dot{\Omega}_E\alpha_E \qquad (7)$$

Equation (7) provides us with tilt-ring laser coupling to be calculated as a function of co-seismic tilts and ring laser location. We note that, to calculate exactly tilt-ring laser coupling, together with (7) equations (A1-9) need to be applied. With small co-seismic tilts, instead of (A1-9) equations (A1-10) can be used and the scale factors in (7) are approximated as follows:

$$\left[\alpha_P - \sin(\Lambda)\right] \approx -\Omega_E \cos\left(\Lambda - \frac{\Omega_E}{2}\right) \qquad (8a)$$

$$\left(\alpha_Z - 1\right) \approx 0 \qquad (8b)$$

$$\alpha_N \approx -\Omega_E \qquad (8c)$$

$$\alpha_E \approx -\Omega_N \qquad (8d)$$

In the following we investigate tilt-ring laser coupling for observations of local earthquakes and tele-seismic events in connection with the corresponding vertical rotation rate.

Observations of local earthquakes

In this section we investigate the tilt coupling that local earthquakes may induce. We first start with the local magnitude scale:

$$M_L = \log (A) - \log (A_O) \quad (9)$$

where A is the maximum trace amplitude (in millimeters) recorded on a standard short-period seismometer (Wood-Anderson instrument) and $\log (A_O)$ is the calibration function and can be calculated as a function of hypocentral distance Δ (in km) for Southern California as follows (Hutton and Boore, 1987):

$$-\log(A_O) = 1.110\log(\Delta/100) + 0.00189(\Delta-100) + 3.0 \quad (10)$$

With the magnification factor of the Wood-Anderson instrument being 2080 (see Booth, 2007), from equation (9) and (10) we can estimate the maximum displacement A_L (in meters) that an earthquake magnitude M_L may induce:

$$A_L = 10^{(M_L + \log A_O - 3)} / 2080 \quad (11)$$

As introduced by Li et al. (2001), in a homogeneous half space the y-component of the co-seismic tilt induced by plane harmonic P and SV waves with the propagation direction in the vertical (x, z) plane can be calculated from the corresponding vertical displacement D_Z by:

- P wave: $$\Omega_y^P = i\omega \frac{\sin\theta_P}{\alpha} D_Z \quad (12)$$

- SV wave: $$\Omega_y^{SV} = i\omega \frac{\sin\theta_{SV}}{\beta} D_Z \quad (13)$$

where $\omega=2\pi/T$, T, θ_P, and θ_{SV}, respectively, are frequency, period, and incident angles of P and SV waves; α and β are P and S wave velocities and D_Z is the vertical displacement.

In fact, scattered SV waves generated by 3D effects may be involved randomly in the P coda. Moreover, both P and SV waves are predominant in a vertical component. Thus, the separation of P and SV wave types is difficult. To simplify calculations, we consider the maximum tilt to be caused by both P and SV waves. Such maximum tilt can be inferred from equations (12) and (13) by taking sines of the incident angles with maximum value being 1, wave velocities with minimum value being β:

$$\Omega_{y\text{-}max}^{P\_SV} = i\frac{2\pi}{T\beta} D_Z \quad (14)$$

Equation (14) indicates that at a given period $\Omega_{y\text{-}max}^{P\_SV}$ reaches the maximum amplitude when D_Z reaches the maximum displacement:

$$\Omega_{y\text{-}max}^{P\_SV} = \frac{2\pi}{T\beta} D_{Z-max} \quad (15)$$

Assuming that the maximum displacement extracted from local magnitude scale is a representative for vertical displacement (e.g. of SV) and let T = 0.8s (period of the

Wood-Anderson instrument), from (11) and (15) we can estimate the maximum tilt (in rad) induced by a local earthquake of magnitude M_L as follows:

$$\Omega_{y\text{-}max}^{M_L} = \frac{\pi}{832\beta} 10^{(M_L + \log A_O - 3)} \qquad (16)$$

Equation (16) provides us with the maximum transverse tilt to be expected in the domain of local magnitude and distance range. Using this equation, maximum co-seismic tilts on bed rock site (β = 3200 m/s) and on soft sediment site (β = 500 m/s) are calculated for the applicable range of local magnitude. The results are present in Figures 1 and 3 (left axes). We can see that in the applicable range of local magnitudes (M_L < 7) and distance (10km ≤ Δ ≤ 600 km) for both types of ground condition (sediment and bed rock) the maximum tilt motion is about 10^{-3} rad. This implies that the use of approximations (A1-10) and (8) in this section is well accepted and (7) can be re-written by:

$$\dot{\Omega}_{Tilt} \approx -\Omega_E \dot{\Omega}_P \cos\left(\Lambda - \frac{\Omega_E}{2}\right) - \Omega_E \dot{\Omega}_N - \Omega_N \dot{\Omega}_E \qquad (17)$$

In theory, P and SV waves coming with a back azimuth φ cause no tilt motion for the radial component. Thus, with the maximum transverse tilt provided by (16) we can calculate the corresponding NS and EW components of tilts as follows (see Appendix 2):

$$\Omega_N = -\Omega_{y\text{-}max}^{M_L} \sin(\varphi) \tag{18}$$

$$\Omega_E = \Omega_{y\text{-}max}^{M_L} \cos(\varphi) \tag{19}$$

The corresponding components of maximum tilt rates (in rad/s) can be estimated using plane wave assumption:

$$\dot{\Omega}_N = \frac{2\pi}{T}\Omega_N = -\frac{2\pi}{T}\Omega_{y\text{-}max}^{M_L} \sin(\varphi) \tag{20}$$

$$\dot{\Omega}_E = \frac{2\pi}{T}\Omega_E = \frac{2\pi}{T}\Omega_{y\text{-}max}^{M_L} \cos(\varphi) \tag{21}$$

Combining (16), (17), (18), (19), (20), and (21), and let $\cos\left(\Lambda - \frac{\Omega_E}{2}\right)\cos(\varphi)$ in the first term with minimum value being -1, $\sin(\varphi)\cos(\varphi) = \frac{\sin(2\varphi)}{2}$ in the second term with maximum value being 0.5, T = 0.8s, we obtain the maximum tilt coupling $\dot{\Omega}_{Tilt}^{max}$ (in rad/s) as a function of magnitude and distance as follows:

$$\dot{\Omega}_{Tilt}^{max} = \dot{\Omega}_P \frac{\pi}{832\beta} 10^{(M_L + \log A_O - 3)} + \frac{\pi^3}{276889.6\beta^2} 10^{2(M_L + \log A_O - 3)} \tag{22}$$

We estimate the maximum value of the corresponding vertical rotation rate to compare with the above tilt coupling. Assuming that A_L is representative of SH-wave

amplitudes, the corresponding peak rotation rate (in rad/s) can be estimated by using the relationship between displacement and rotation rate (see Igel et al. 2007):

$$\dot{\Omega}_Z = 2\frac{\pi^2}{\beta T^2} A_L = \frac{\pi^2}{665.6\beta} 10^{(M_L + \log A_O - 3)} \qquad (23)$$

Equations (22), and (23), respectively, provide us with maximum tilt-ring laser coupling and vertical rotation rate to be expected in the domain of local magnitude and distance range. We use these equations to investigate the expected values for two cases: bed rock with β = 3200 m/s and soft sediment with β = 500 m/s. The results are presented in Figures 1, 2 (for bed rock) and 3, 4 (for soft sediment).

The figures show the maximum values to be expected as a function of distance for different magnitudes (left) and as a function of magnitude for different distances (right). We can see that in the applicable range of local magnitudes (M_L < 7) and distance (10km $\leq \Delta \leq$ 600 km) for both types of ground condition (sediment and bed rock), at the same distance the increase one unit of magnitude leads to the enlargement of about one order of amplitude of tilt and rotation rate. The same tendency is shown for tilt-ring laser coupling at large distance with small magnitude (weak motions). However, at the same distance close to source with large magnitude (strong motions) the raise of one unit of magnitude results in the increase of about two orders of amplitude of tilt-ring laser coupling. The maximum tilt-ring laser coupling predicted for sediment site is two orders of magnitude bigger than corresponding one on the bed rock. Nevertheless, maximum tilt-ring laser coupling predicted for both sites (Figures 2 and 4) is at least two orders of

magnitude smaller than the corresponding maximum rotation rate (right axes of Figures 1 and 3) and therefore can be neglected.

We note that for strong motions at near source, $\dot{\Omega}_Z$, $\dot{\Omega}_N$, and $\dot{\Omega}_E$ may reach amplitudes on the order of 10^{-2} rad/s (Nigbor, 1994) or greater. This implies that they are much more significant than $\dot{\Omega}_P$ with magnitude order of 10^{-5} rad/s. As a consequence, contribution of the first term in equation (7) can be ignored and the ring laser location virtually has no effect. In this case, both horizontal components of seismically induced rotations play the same role on affecting ring laser measurements. At this point it should be noted that ring laser technology is unlikely to play a major role for near source observations. Nevertheless other technologies (e.g. fiber-optic approaches) need to be investigated for cross-axis sensitivity in a similar way.

Observations of tele-seismic events

For tele-seismic events $\dot{\Omega}_P$ are much more significant than $\dot{\Omega}_Z$, $\dot{\Omega}_N$, and $\dot{\Omega}_E$ (order of 10^{-8} rad/s for large earthquakes - see Igel et al. 2007; Pham et al. 2008). In this case, with scale factors mentioned through equations (8), the significant part of tilt - ring laser coupling comes from the first term in (7). Thus:

$$\dot{\Omega}_{Tilt} = -\dot{\Omega}_P \Omega_E \cos\left(\Lambda - \frac{\Omega_E}{2}\right) \qquad (24)$$

Equation (24) implies that for observations of tele-seismic events the tilt coupling depends on the location of the ring laser and Ω_E only. With the same tilt motion, the tilt coupling reaches a maximum when $\Lambda = \Omega_E / 2$ (ring laser is almost at the equator) and minimum when $\Lambda = 90$ deg (ring laser at the pole).

We use (24) to investigate the variations of maximum tilt coupling that tele-seismic events may induce. We start with the IASPEI formula of the surface wave magnitude:

$$M_S = \log (A_S/T) + 1.66 \log D + 3.3 \qquad (25)$$

where A_S is the peak ground amplitude (in micrometers) of the surface (Rayleigh) wave in the vertical component within the period range $18s \le T \le 22s$, and D is epicentral distance (in degree) in the range $20^0 \le D \le 160^0$.

From (25), Rayleigh waves of an earthquake magnitude M_S are expected to induce a maximum vertical displacement (in meters):

$$A_S = T.10^{(M_S - 1.66 \log D - 9.3)} \qquad (26)$$

According to Li et al. (2002), the co-seismic tilt induced by a Rayleigh wave in a homogeneous half space can be calculated from its vertical displacement D_Z by:

$$\Omega_y^R = i\frac{\omega}{V_R} D_Z \tag{27}$$

where $\omega=2\pi/T$ and V_R are frequency and Rayleigh wave phase velocity, respectively.

Equation (27) indicates that with a certain value of the phase velocity at a given period, Ω_y^R reaches the peak value when D_Z reaches a peak displacement A_S:

$$\Omega_{y-\max}^R = \frac{2\pi}{TV_R} A_S \tag{28}$$

Combining (26) and (28), the maximum tilt (in rad) induced by an earthquake magnitude M_S thus is:

$$\Omega_{y-\max}^R = \frac{2\pi}{V_R} 10^{(M_S - 1.66\log D - 9.3)} \tag{29}$$

This $\Omega_{y-\max}^R$ will cause maximum tilt coupling $\dot{\Omega}_{Tilt-\max}^R$ (in rad/s) if it plays the role of -Ω_E in equation (24) and $\cos\left(\Lambda - \frac{\Omega_E}{2}\right)$ obtains its maximum value being 1:

$$\dot{\Omega}_{Tilt-\max}^R = \dot{\Omega}_P \frac{2\pi}{V_R}.10^{(M_S - 1.66\log D - 9.3)} \tag{30}$$

Equations (29) and (30) provide us with the maximum tilt and tilt coupling to be expected in the domain of applicable surface wave magnitude and distance range. Taking V_R = 3100 m/s for a dominant period of T = 20s such expected maximum values are calculated and presented in Figure 5. The figure shows the maximum values to be expected as a function of distance for different magnitudes (left) and as a function of magnitude for different distances (right). The left axes denote the expected tilt in rad and right axes denote the expected tilt coupling in rad/s. Compared to the corresponding predicted rotation rate shown in Igel et al. (2007) the expected tilt coupling is three orders of magnitude smaller and can be ignored.

Tilt - ring laser coupling: observations in the P coda

As reported by Igel et al. (2007) and Pham et al. (2008), there are significant high frequency motions of vertical component of rotations in the P coda of tele-seismic signals. This type of signals is either directly visible or can be inferred through the investigation of cross-correlation between transverse acceleration and vertical rotation rate. A typical example for this phenomenon is shown in Figure 6 for the Tokachi-oki event 25/9/2003 M8.1 (see Pham et al. 2008 for more details). Theoretically, in spherically symmetric isotropic media we should not observe a vertical component of rotation before the onset of SH waves. One of possible explanations for the observed P coda rotations is tilt-ring laser coupling. These observations were part of the motivation for the present study aiming at the first quantitative estimates of tilt-ring laser coupling in

connection with tele-seismic observations. In this section we focus on investigating the effects of tilt-ring laser coupling in the observed P coda. The aim is to give a quantitative answer to the question, whether tilt-ring laser coupling contributes to the rotational motions observed in the P coda. The magnitude-amplitude relations previously used in the general case do not apply in this case which is why we estimate the tilt-coupling effects directly from the data.

As shown in the previous section, the calculation of tilt-ring laser coupling requires knowledge of the horizontal components of seismically induced rotations (or tilts). However, tiltmeters - sensors measuring horizontal components of rotational motions at the Earth's surface - are sensitive to translation motions, and therefore do not provide the correct tilt signals in the required frequency band (Suryanto, 2006). Here we investigate the effects of tilt-ring laser coupling in the observed P coda based on translation derived tilts (see Li et al. 2001).

We apply equation (14) to derive maximum co-seismic tilt in the P coda from observed translations and use it to quantify the corresponding tilt-ring laser coupling. It should be noted that Li's equations are developed under the assumption of harmonic plane waves (Li et al. 2001) and a homogeneous half space. Thus, to derive tilt signal we first convert the time series of displacements to harmonic discrete frequencies by Fourier transformation. We use equation (14) to define the Fourier spectra of the transverse tilt at discrete frequencies as a function of the Fourier spectra of the displacement. The time history of the transverse tilt finally can be obtained by inverse Fourier transformation.

As mentioned by Trifunac et al. (2001), Graizer (2005, 2006) and Pillet et al. (2007) standard measurements of translations are contaminated by co-seismic rotations. Fortunately, this type of contamination is negligible at high frequencies for far field observations. Thus, at high frequencies considered in this study the observed translations are applicable to derive tilt motions.

The observed seismograms of the Tokachi-oki 25-09-2003 M8.1 earthquake are used to investigate tilt-ring laser coupling in the P coda (see Data and Resources Section). The vertical component of the observed velocities of the event is high pass filtered with cut-off period 150s then integrated to obtain displacement. This signal is used to derive the corresponding maximum tilt motion. The translation derived tilt is then applied as the role of the Ω_E in equation (24) to estimate the corresponding tilt-ring laser coupling. The result is presented in Figure 7 (third trace from top). It is three orders of magnitude smaller than the corresponding rotation rate measured by the ring laser sensor, thus the tilt coupling in the P coda of the event is insignificant. In addition, after subtracting this estimated tilt coupling, the P coda rotations are still visible (Figure 7, fourth trace from top). We calculate zero lag normalized cross correlation coefficients between the transversal acceleration and the corrected P coda rotations for a 2s sliding window after high-pass filtering both signals with cut off period 1s. The results show a pronounced increases right after the P wave onset (Figure 7, bottom). All these results indicate that for the observations of the Tokachi-oki 25-09-2003 M8.1 event the tilt-ring laser coupling is insignificant and can be ignored.

We finally use the available database of events observed by both the broad-band-seismometer and the ring laser sensor at Wettzell station (see Data and Resources Section) to examine systematically maximum tilt-ring laser coupling in the P coda by comparing it with corresponding observed peak rotation rate. Events of Algeria 21-05-2003 M6.9, Tokachi-oki 25-09-2003 M8.1, Russia 27-09-2003 M7.5, and Sumatra 12-09-2007 M8.4 were chosen for this study because they are distributed in different ranges of magnitude, distance, and back azimuth and their P coda rotations are clearly visible (see Pham et al. 2008). Since the observed P coda rotations are predominant around a period of 1s (Pham et al. 2008), the vertical displacements and the observed rotation rates of these events are filtered in a narrow band with central period 0.5s, 1s, and 2s, then peak values were extracted. We use equation (15) to calculate maximum co-seismic tilt then use it as Ω_E in equation (24) to calculate the maximum tilt-ring laser coupling in the P coda. The results are presented in Table 1. We can recognize that for all considered events and periods the predicted tilt-ring laser coupling is four orders of magnitude smaller than observed peak rotation rate. We conclude that tilt-ring laser coupling in the P coda is negligible and the main causes for the observed P coda rotations thus should come from 3D effects (e.g. P-SH scattering, as suggested by Pham et al., 2008).

Discussions and conclusions

Previously, several authors reported about effects of co-seismic tilts on ring laser measurements (e.g. McLeod et al. 1998; Schreiber et al. 2005, 2006). However, these studies did not fully quantify the effects and discuss the relevance for broad band ring laser data processing. The main goal of this study is to fill this gap and investigate quantitatively the effects of co-seismic tilts on ring laser measurements.

In this paper, we present equations of cross-axis sensitivity for ring laser sensors. To calculate tilt-ring laser coupling requires knowledge of horizontal components of seismically induced rotations (or tilts). Nevertheless, measurements of co-seismic tilt using tiltmeters provide incorrect signals in the frequency band of interest because of the sensitivity of tiltmeters to horizontal accelerations (e.g., Suryanto 2006). We perform estimates of maximum tilt-ring laser coupling based on magnitude-amplitude relations to be expected for observations of local earthquakes and tele-seismic events. The results show negligible tilt coupling for all the applicable range of the surface wave magnitude and local magnitude scales.

Because ring laser technology is unlikely to play a major role for near source observations and since the appearance of the ring laser rotational signals in the P coda of the tele-seismic events (Igel et al. 2007, Pham et al. 2008) need to be explained, our investigations on data-based tilt-ring laser coupling focus on the P coda observations. Translation derived tilt (Li et al. 2001) is applied to observed translations to estimate the maximum tilt-ring laser coupling for P coda at high frequencies. The results obtained again show that the tilt-ring laser coupling can be neglected.

In summary, it can be concluded that tilt-ring laser coupling is negligible compared to the corresponding vertical rotation rate not only for observations of tele-seismic events but also for all the applicable range of the local magnitude scale.

Data and Resources

The observed seismograms of period 2003-2004 used in this study were provided by the Geophysics Section, Ludwig Maximilians University Munich and published by Igel et al. (2007). The translational and rotational seismograms of the events that occurred after September of 2007 can be obtained from the WebDC - Integrated Seismological Data Portal at http://www.webdc.eu/arclink/query?sesskey=0841ed49.

Acknowledgments

The research was supported by the Geophysics Section - LMU Munich, the Vietnamese Government (Project 322), and the German Academic Exchange Service (DAAD). We acknowledge the contributions of the Bundesamt für Kartographie und Geodäsie (BKG) towards the installation and operation of the ‘G’ ring laser at the geodetic observatory Wettzell. We thank the KONWIHR project and the Munich Leibniz Supercomputing Centre for computational resources, and the European Human Resources

Mobility Program (SPICE project). Thanks to Josep de la Puente for discussion and comments.

References

Booth, D.C. An improved UK local magnitude scale from analysis of shear and Lg-wave amplitudes, *Geophys. J. Int.*, 169, 593-601, doi: 10.1111/j.1365-246X.2006.03324.x (2007).

Cochard, A., Igel, H., Schuberth, B., Suryanto, W., Velikoseltsev, A., Schreiber, U., Wassermann, J., Scherbaum, F., Vollmer, D. Rotational motions in seismology: theory, observations, simulation, in "*Earthquake source asymmetry, structural media and rotation effects*" eds. Teisseyre et al. Springer Verlag (2006).

Fichtner A. and Igel H., Sensitivity densities for rotational ground motion measurements, *Bull. Seism. Soc. Amer.*, this issue, (2008).

Graizer, V. M. Effect of tilt on strong motion data processing, Soil Dyn. Earthq. Eng, 25, 197-204 (2005).

Graizer, V. M. Equation of pendulum motion including rotations and its implications to the strong-ground motion, in Earthquake Source Asymmetry, Structural Media and Rotation Effects, 471-491 (2006).

Hutton, L. K., Boore, D.M. The M_L scale in Southern California, *Bull. Seism. Soc. Amer.,* 77, 2074-2097 (1987).

Igel, H., Cochard, A., Wassermann, J., Flaws, A., Schreiber, U., Velikoseltsev, A., Pham, D.N. Broadband observations of earthquake induced rotational ground motions, *Geophys. J. Int.*, 168, 182-196, doi: 10.1111/j.1365-246X.2006.03146x (2007).

Igel, H., Schreiber, K.U., Flaws, A., Schuberth, B., Velikoseltsev, A., Cochard, A. Rotational motions induced by the M8.1 Tokachi-oki earthquake, September 25, 2003, *Geophys. Res. Lett.*, 32, L08309, doi:10.1029/2004GL022336 (2005).

Li, H., Sun, L., Wang, S. Improved approach for obtaining rotational components of seismic motion. *Transactions*, SmiRT 16, 1-8 (2001).

Li, H., Sun, L., Wang, S. Frequency dispersion characteristics of phase velocities in surface wave for rotational components of seismic motion. *Journal of Sound and Vibration*, 258 (5), 815-827 (2002).

McLeod, D.P., Stedman, G.E., Webb, T.H. & Schreiber, U. Comparison of standard and ring laser rotational seismograms. *Bull. Seism. Soc. Amer.* 88, 1495-1503 (1998).

Nigbor R. L. Six-degree-of-freedom ground-motion measurement. *Bull. Seism. Soc. Amer.,* 84, 1655-1669 (1994).

Pancha, A., Webb, T.H., Stedman, G.E., McLeod, D.P. & Schreiber, U. Ring laser detection of rotations from teleseismic waves. *Geophys. Res. Lett*. 27, 3553-3556 (2000).

Pham D.N., Igel H., Wassermann, J., M. Käser, J. de la Puente, Schreiber, U. Observations and modelling of rotational signals in the P-Coda: constraints on crustal scattering, *Bull. Seism. Soc. Amer.*, this issue, (2008).

Pillet R. and Virieux J. The effects of seismic rotations on inertial sensors, *Geophys. J. Int.*, doi: 10.1111/j.1365-246X.2007.03617.x (2007).

Schreiber, U., Igel, H., Cochard, A., Velikoseltsev, A., Flaws, A., Schuberth, B., Drewitz, W., Müller, F., The GEOsensor project: A new observable for seismology. In "Observation of the System Earth from Space", Springer (2005).

Schreiber, U., Stedman, G.E., Igel, H., Flaws, A. Ring laser gyroscopes as rotation sensors for seismic wave studies. In "*Earthquake source asymmetry, structural media and rotation effects*" eds. Teisseyre et al., Springer Verlag (2006).

Schreiber, K.U., J. N. Hautmann, J.N., Velikoseltsev A., J. Wassermann J. , Igel H., Otero J., Vernon, F., and Well s, J.P.R., Ring Laser Measurements of Ground Rotations for Seismology, *Bull. Seis. Soc. Amer.*, this issue, submitted.

Suryanto W., Igel H., Wassermann J., Cochard A., Schuberth B., Vollmer D., Scherbaum F., Schreiber U., and Velikoseltsev A.. First comparison of array-derived rotational ground motions with direct ring laser measurements, *Bull. Seis. Soc. Amer.,* 96, 2059-2071 (2006).

Suryanto W. Rotational motions in seismology, theory and application. PhD. Dissertation, LMU Munich (http://edoc.ub.uni-muenchen.de/7850/), (2006).

Trifunac, M.D. & Todorovska, M.I. A note on the usable dynamic range of accelerographs recording translation. *Soil Dyn. and Earth. Eng*. 21(4), 275-286 (2001).

Authors affiliations, addresses

Nguyen Dinh Pham[*], Heiner Igel, Joachim Wassermann

Geophysics Section,

Department of Earth and Environmental Sciences,

Ludwig Maximilians Universität München,

Theresienstrasse 41,

80333 München, GERMANY.

Alain Cochard

Ecole et Observatoire des Sciences de laTerre,

Institut de Physique du Globe,

5 rue Ren´e Descartes, F-67084 Strasbourg Cedex, FRANCE.

Ulrich Schreiber

Forschungseinrichtung Satellitengeodäsie,

Technical University Munich,

Fundamentalstation Wettzell, Sackenriederstrasse 25,

D-93444 *Kötzting, GERMANY.*

(*) Institute of Geophysics,

Vietnamese Academy of Science and Technology,

18 Hoang Quoc Viet, Cau Giay, Hanoi, VIETNAM.

Table 1. Observations and maximum tilt and tilt coupling at different dominant periods in the P coda of the typical events

Event	Observed peak Dz (nm)			Observed peak $\dot{\Omega}_Z$ (nrad/s)			Maximum tilt (nrad)			Maximum tilt coupling (10^{-5} nrad/s)		
	0.5 (s)	1 (s)	2 (s)	0.5 (s)	1 (s)	2 (s)	0.5 (s)	1 (s)	2 (s)	0.5 (s)	1 (s)	2 (s)
Algeria 21-05-2003, M6.9	84.40	329.31	631.52	0.14	0.30	0.11	0.31	0.61	0.58	1.50	2.94	2.81
Tokachi-oki 25-09-2003, M8.1	199.52	355.78	1235.37	0.52	0.63	0.44	0.73	0.66	1.14	3.56	3.17	5.51
Russia 27-09-2003, M7.5	73.40	366.53	638.02	0.40	0.46	0.37	0.27	0.68	0.59	1.31	3.27	2.84
Sumatra 12-09-2007, M8.4	75.74	309.34	1353.02	0.07	0.30	0.51	0.28	0.57	1.25	1.35	2.76	6.03

Figure Captions

Figure 1. Maximum tilt (left axes) and vertical rotation rate (right axes) are predicted for a dominant period T = 0.8s on the bed rock (β = 3200 m/s) as a function of local magnitude and hypocentral distance.

Figure 2. Maximum tilt-ring laser coupling is predicted for a dominant period T = 0.8s on the bed rock (β = 3200 m/s) as a function of local magnitude and hypocentral distance.

Figure 3. Maximum tilt (left axes) and vertical rotation rate (right axes) are predicted for a dominant period T = 0.8s on the soft sediment (β = 500 m/s) as a function of local magnitude and hypocentral distance.

Figure 4. Maximum tilt-ring laser coupling is predicted for a dominant period T = 0.8s on the soft sediment (β = 500 m/s) as a function of local magnitude and hypocentral distance.

Figure 5. Expected maximum tilt (left axes) and tilt-ring laser coupling (right axes) induced by tele-seismic Rayleigh waves as a function of surface wave magnitude and distance. Phase velocity is assumed V_R = 3100 m/s.

Figure 6. Observations of the Tokachi-oki event 25-09-2003, M8.1 at the Wettzell station. Top three traces: Vertical acceleration, transverse acceleration and rotation rate, respectively. Bottom: zero lag normalized cross correlation coefficients between rotation rate and transverse acceleration after high-pass filtering with cut-off period 1s, calculated for 2s sliding time windows. The figure shows significant rotational motions in the P coda.

Figure 7. Seismic signals in the P coda of the Tokachi-oki event 25-09-2003, M8.1. Two top traces: vertical (A_Z) and transverse (A_T) components of accelerations; The third trace from top: the maximum tilt-ring laser coupling derived from translation; The fourth trace from top: observed rotation rate after subtracting the maximum tilt-ring laser coupling; Bottom: variations of the correlation coefficients between the corrected rotation rate and transverse acceleration.

Figure A1. Illustration of ring laser location on the Earth's surface

Figure A2. A ring laser sensor is tilted and shifted by seismic waves. O{0,0,0} is the original location of the ring laser. R{Δx, Δy , Δz} is new location of the ring laser under the effects of seismic wave. R_1 is chosen in the line of intersection between the ring laser plane and xOz plane with distance $RR_1 = 1$. R_2 is chosen in the line of intersection between the ring laser plane and yOz plane with distance $RR_2 = 1$.

Figure A3. Axis transformations of tilts

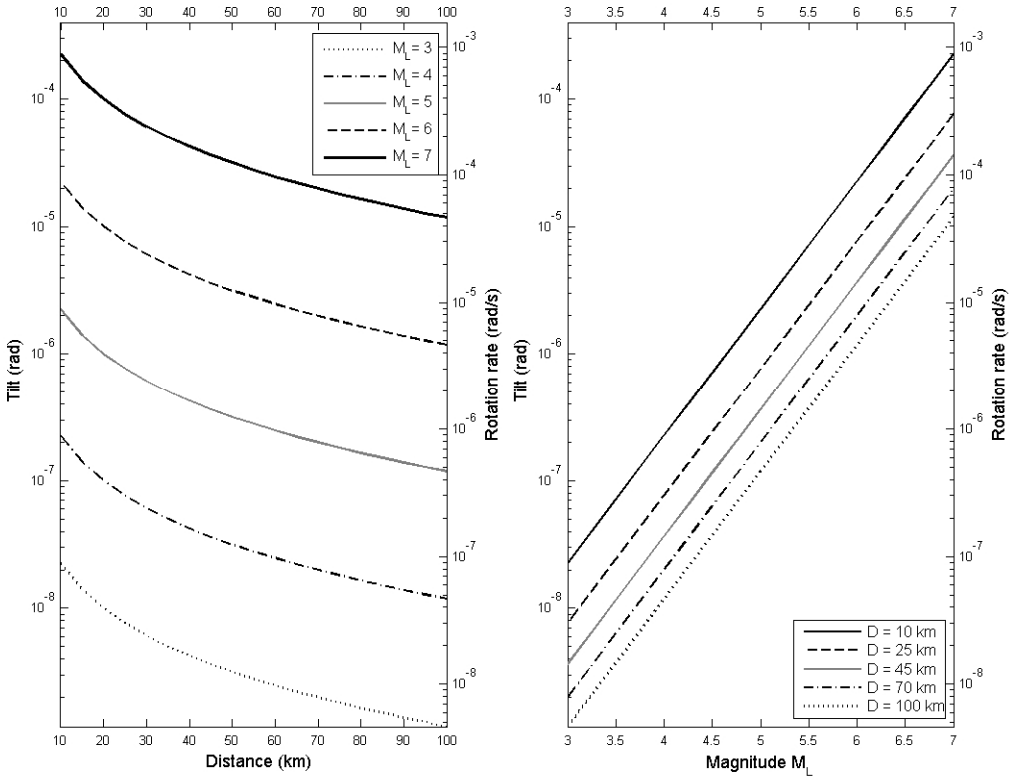

Figure 1. Maximum tilt (left axes) and vertical rotation rate (right axes) are predicted for a dominant period $T = 0.8$s on the bed rock ($\beta = 3200$ m/s) as a function of local magnitude and hypocentral distance.

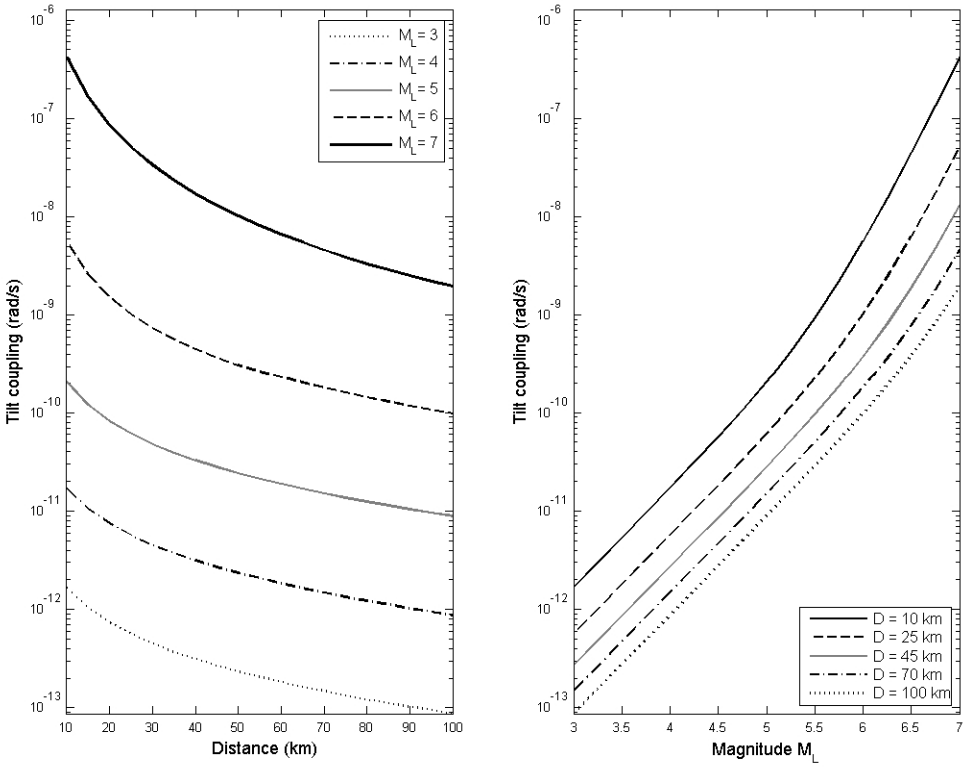

Figure 2. Maximum tilt-ring laser coupling is predicted for a dominant period $T = 0.8$s on the bed rock (β = 3200 m/s) as a function of local magnitude and hypocentral distance.

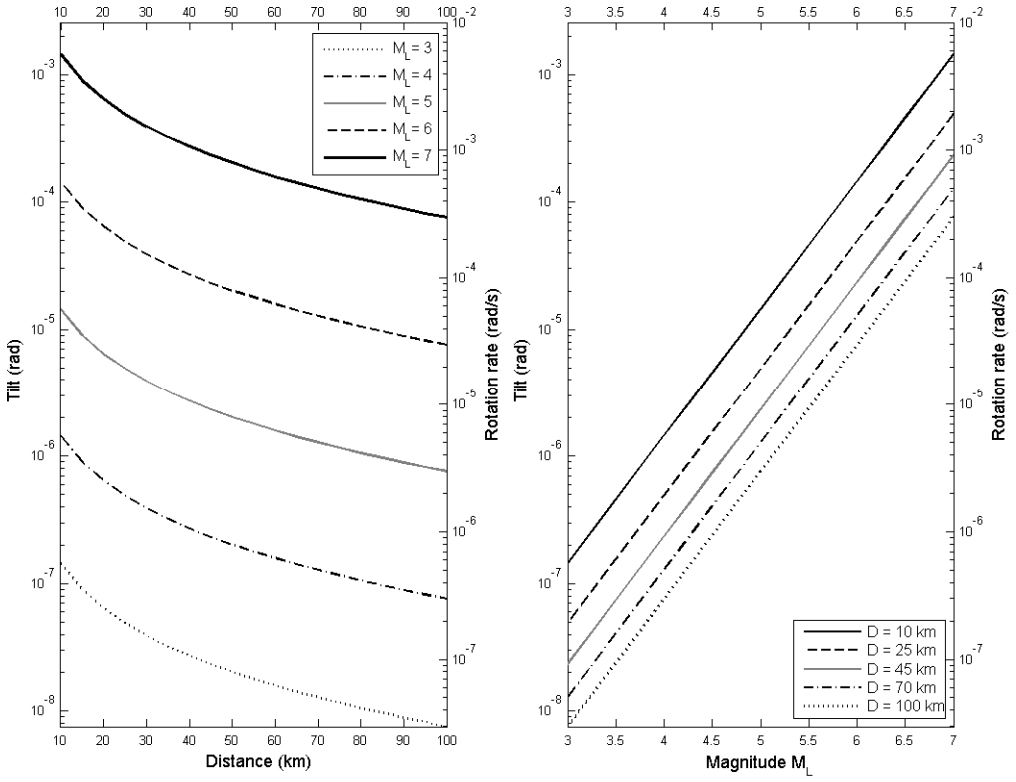

Figure 3. Maximum tilt (left axes) and vertical rotation rate (right axes) are predicted for a dominant period T = 0.8s on the soft sediment (β = 500 m/s) as a function of local magnitude and hypocentral distance.

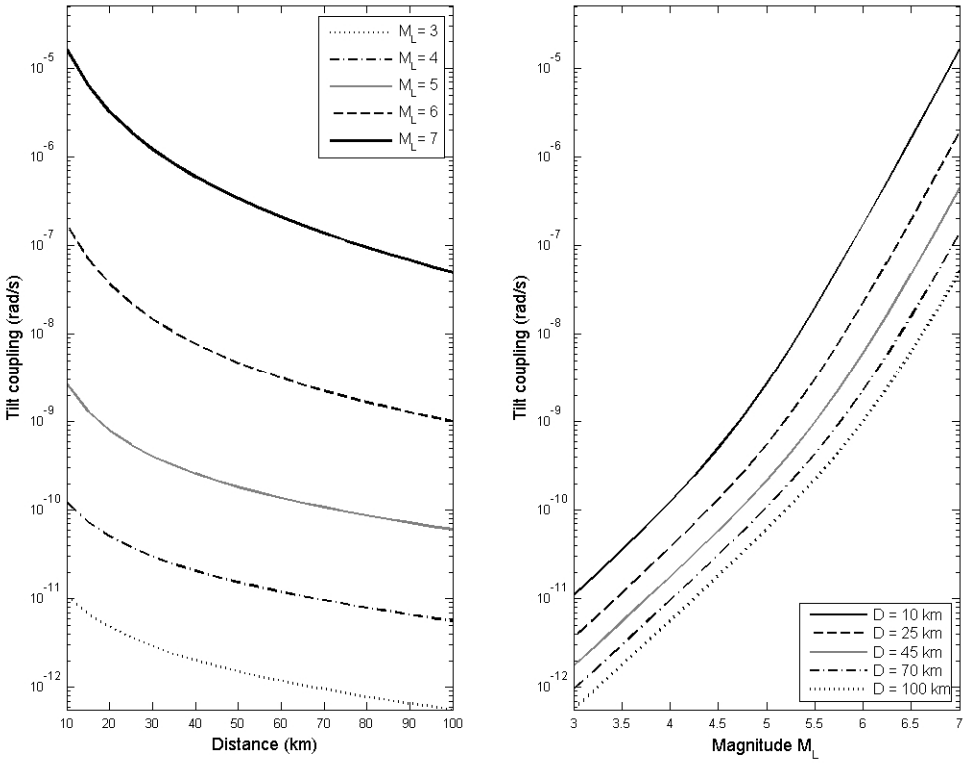

Figure 4. Maximum tilt-ring laser coupling is predicted for a dominant period $T = 0.8$s on the soft sediment ($\beta = 500$ m/s) as a function of local magnitude and hypocentral distance.

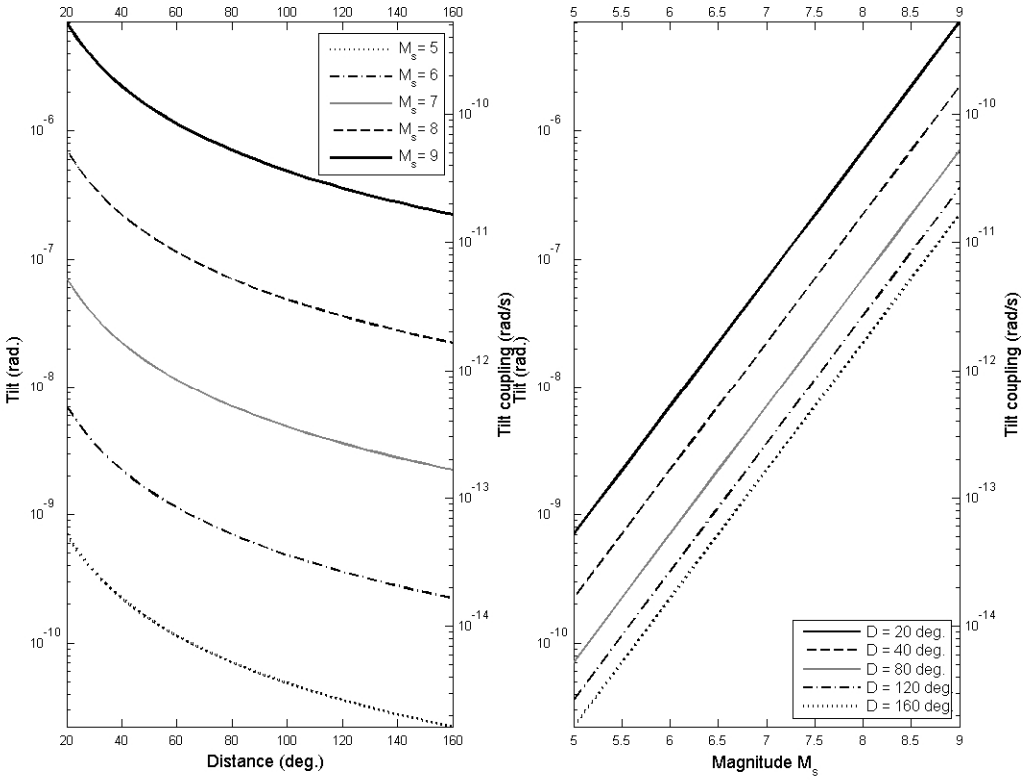

Figure 5. Expected maximum tilt (left axes) and tilt-ring laser coupling (right axes) induced by tele-seismic Rayleigh waves as a function of surface wave magnitude and distance. Phase velocity is assumed V_R = 3100 m/s.

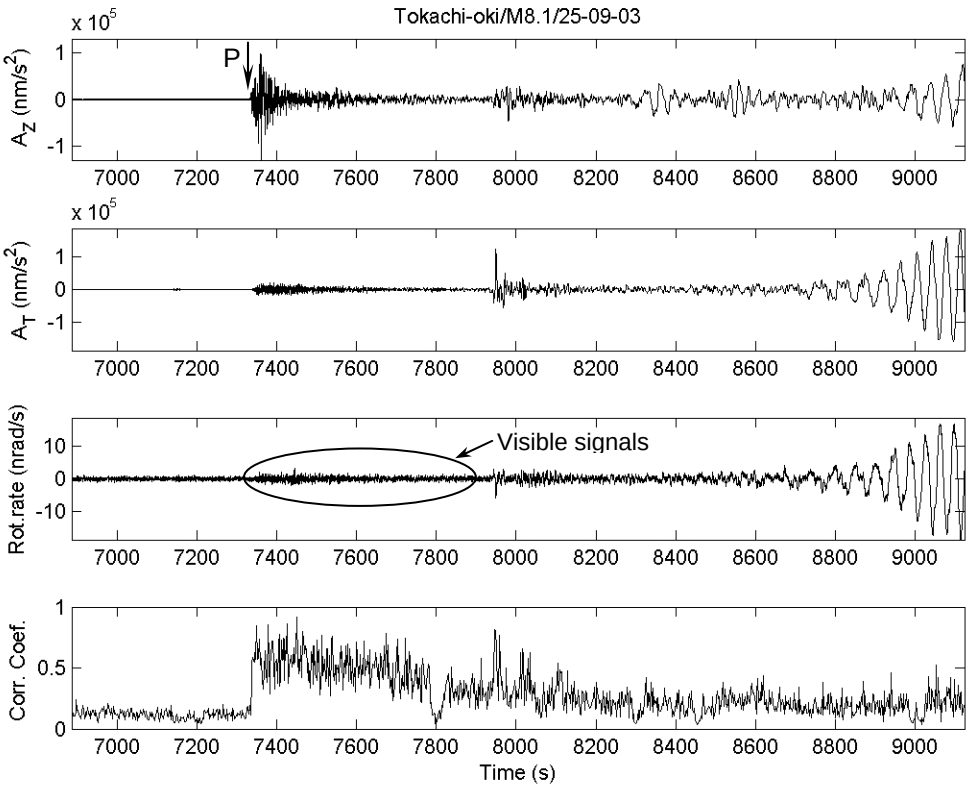

Figure 6. Observations of the Tokachi-oki event 25-09-2003, M8.1 at the Wettzell station. Top three traces: Vertical acceleration, transverse acceleration and rotation rate, respectively. Bottom: zero lag normalized cross correlation coefficients between rotation rate and transverse acceleration after high-pass filtering with cut-off period 1s, calculated for 2s sliding time windows. The figure shows significant rotational motions in the P coda.

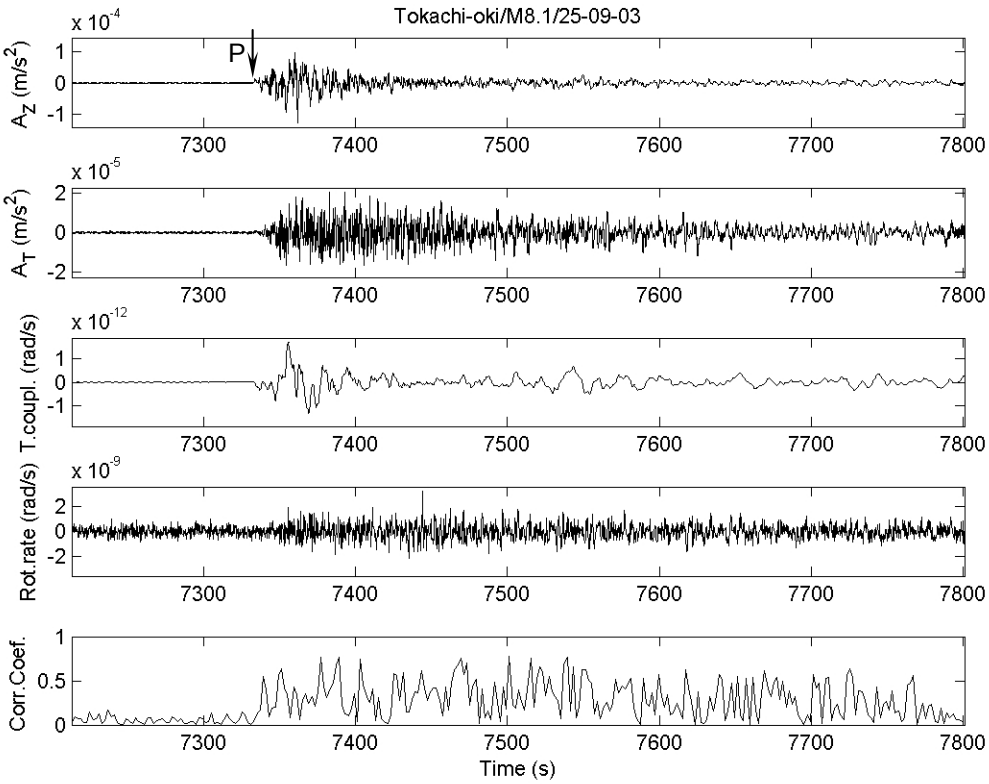

Figure 7. Seismic signals in the P coda of the Tokachi-oki event 25-09-2003, M8.1. Two top traces: vertical (A_Z) and transverse (A_T) components of accelerations; The third trace from top: the maximum tilt-ring laser coupling derived from translation; The fourth trace from top: observed rotation rate after subtracting the maximum tilt-ring laser coupling; Bottom: variations of the correlation coefficients between the corrected rotation rate and transverse acceleration.

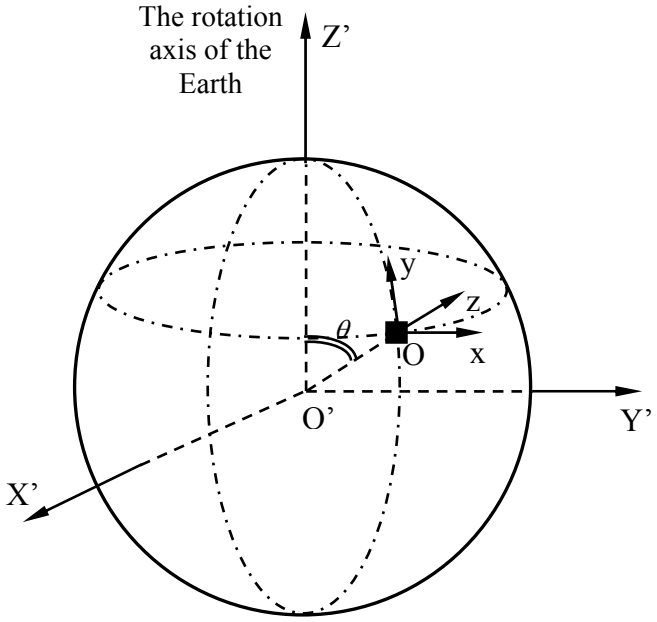

Figure A1. Illustration of ring laser location on the Earth’s surface

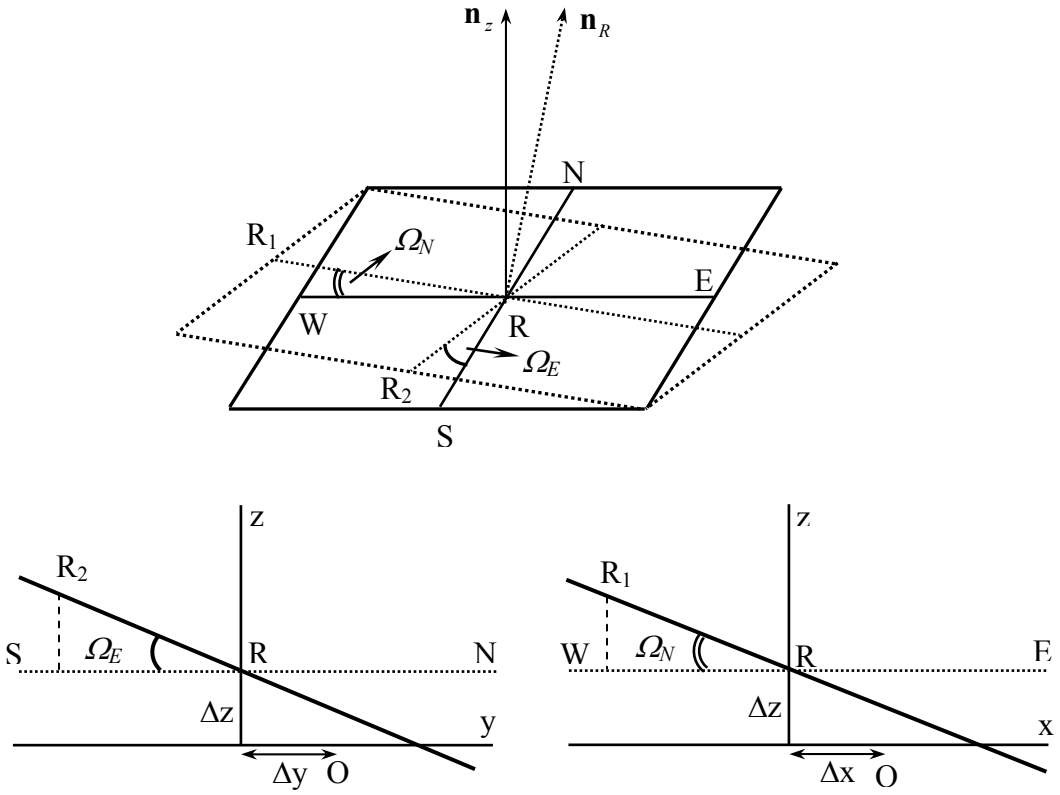

Figure A2. A ring laser sensor is tilted and shifted by seismic waves. O{0,0,0} is the original location of the ring laser. R{Δx, Δy , Δz} is new location of the ring laser under the effects of seismic wave. R_1 is chosen in the line of intersection between the ring laser plane and xOz plane with distance $RR_1 = 1$. R_2 is chosen in the line of intersection between the ring laser plane and yOz plane with distance $RR_2 = 1$.

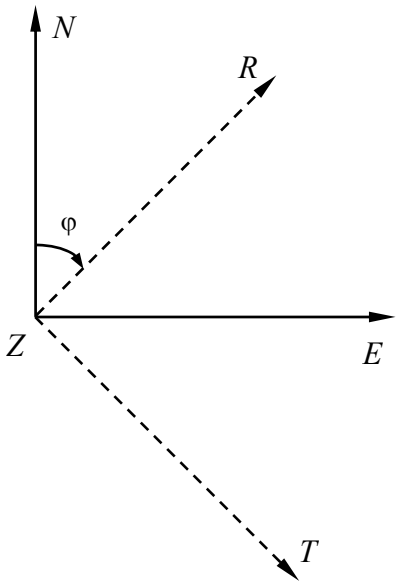

Figure A3. Axis transformations of tilts

Appendix A1: Variations of the normal unit vector of a ring laser

Under the effects of seismic waves, a ring laser may be both tilted and shifted. As a consequence, its normal unit vector $\mathbf{n}_R$ is varied. Here we quantify this variation through cosines of angles between $\mathbf{n}_R$ and the unit basis vectors $\mathbf{n}_P$, $\mathbf{n}_Z$, $\mathbf{n}_N$, $\mathbf{n}_E$ of the rotation axis of the Earth, vertical, NS, and EW axes at the ring laser location, respectively. To do that we locate all the mentioned vectors in the Cartesian coordinate system Oxyz at the original location O of the ring laser, in which Ox, Oy and Oz are respectively corresponding with the local EW, NS, and vertical axes (Figure A1).

$\mathbf{n}_Z$, $\mathbf{n}_N$, and $\mathbf{n}_E$ are defined in Oxyz system by:

$$\mathbf{n}_{Z\ (\mathrm{Oxyz})} = \{0, 0, 1\} \qquad \text{(A1\_1)}$$

$$\mathbf{n}_{N\ (\mathrm{Oxyz})} = \{0, 1, 0\} \qquad \text{(A1\_2)}$$

$$\mathbf{n}_{E\ (\mathrm{Oxyz})} = \{1, 0, 0\} \qquad \text{(A1\_3)}$$

The unit basis vector $\mathbf{n}_P$ of the rotation axis of the Earth at first is considered in another Cartesian coordinate system O'X'Y'Z' (root point O' and O'Z', respectively, are the core point and the rotation axis of the Earth – see Figure A1). In this system, $\mathbf{n}_P$ is determined by:

$$\mathbf{n}_{P\ (\mathrm{O'X'Y'Z'})} = \{0, 0, 1\} \qquad \text{(A1\_4)}$$

On the other hand, let θ and Λ, respectively, denote colatitude and latitude of the original location of the ring laser (Figure A1), we have:

$$\cos(Ox,O'Z') = 0 \qquad \text{(A1\_5a)}$$

$$\cos(Oy,O'Z') = \cos\left(\frac{\pi}{2} - \theta\right) = \cos(\Lambda) \qquad \text{(A1\_5b)}$$

$$\cos(Oz,O'Z') = \cos(\theta) = \sin(\Lambda) \qquad \text{(A1\_5c)}$$

Applying coordinate transformations and using (A1_4), (A1_5) one can infer the $\mathbf{n}_P$ in the Oxyz system:

$$\mathbf{n}_{P\ (Oxyz)} = \{0, \cos(\Lambda), \sin(\Lambda)\} \qquad \text{(A1\_6)}$$

For the normal unit vector $\mathbf{n}_R$ of the ring laser, we locate it from the equation of the ring laser plane in the Oxyz system which can be determined through three non-linear points on the plane (see Appendix A3). Assuming that, when seismic waves arrive the ring laser is moved to a new certain location R $\{\Delta x, \Delta y, \Delta z\}$ in the Oxyz system (Figure A2). The seismically induced tilts of the ring laser sensor about x and y axes themselves are the horizontal components of rotations Ω_E, Ω_N, respectively (Cochard et al. 2006). Together with R, we choose R_1 in the line of intersection between the ring laser plane and xOz plane with distance $RR_1 = 1$, R_2 in the line of intersection between the ring laser plane and yOz plane with distance $RR_2 = 1$ to determine the equation of the ring laser

plane. The coordinates of R_1 and R_2 in the Oxyz system can be easily determined as $R_1\{\cos(\Omega_N)+\Delta x,\ \Delta y,\ \sin(\Omega_N)+\ \Delta z\}$ and $R_2\{\Delta x,\ \cos(\Omega_E)+\Delta y,\ \sin(\Omega_E)+\ \Delta z\}$ (see Figure A2). Hence, the equation of the ring laser plane can be written as follows (Appendix A3):

$$\begin{vmatrix} x-\Delta x & y-\Delta y & z-\Delta z \\ \cos(\Omega_N) & 0 & \sin(\Omega_N) \\ 0 & \cos(\Omega_E) & \sin(\Omega_E) \end{vmatrix} = 0$$

Or:

$$\begin{aligned} &-\cos(\Omega_E)\sin(\Omega_N)x-\sin(\Omega_E)\cos(\Omega_N)y+\cos(\Omega_E)\cos(\Omega_N)z \\ &+\left[\cos(\Omega_E)\sin(\Omega_N)\Delta x+\sin(\Omega_E)\cos(\Omega_N)\Delta y-\cos(\Omega_E)\cos(\Omega_N)\Delta z\right]=0 \end{aligned} \qquad \text{(A1\_7)}$$

Equation (A1_7) implies that changes of location R $\{\Delta x, \Delta y, \Delta z\}$ affect the equation of the ring laser plane, but have no effect to the normal unit vector $\mathbf{n}_R$ that can be inferred as follows (see Appendix A3):

$$\mathbf{n}_{R\ (\text{Oxyz})} = \{n_1, n_2, n_3\} \qquad \text{(A1\_8a)}$$

$$n_1 = \frac{-\cos(\Omega_E)\sin(\Omega_N)}{\sqrt{1-\sin^2(\Omega_E)\sin^2(\Omega_N)}} \qquad \text{(A1\_8b)}$$

$$n_2 = \frac{-\sin(\Omega_E)\cos(\Omega_N)}{\sqrt{1-\sin^2(\Omega_E)\sin^2(\Omega_N)}} \qquad \text{(A1\_8c)}$$

$$n_3 = \frac{\cos(\Omega_E)\cos(\Omega_N)}{\sqrt{1-\sin^2(\Omega_E)\sin^2(\Omega_N)}} \qquad \text{(A1\_8d)}$$

Using (A1_1), (A1_2), (A1_3), (A1_6), and (A1_8), cosine of angles between normal unit vector $\mathbf{n}_R$ of the ring laser and the unit basis vectors $\mathbf{n}_P$, $\mathbf{n}_Z$, $\mathbf{n}_N$, $\mathbf{n}_E$ of the rotation axis of the Earth, vertical, NS, and EW axes at the ring laser location, respectively, are calculated by (see Appendix A3):

$$\alpha_P = \frac{\cos(\Omega_N)\sin(\Lambda - \Omega_E)}{\sqrt{1-\sin^2(\Omega_E)\sin^2(\Omega_N)}} \qquad \text{(A1_9a)}$$

$$\alpha_Z = \frac{\cos(\Omega_E)\cos(\Omega_N)}{\sqrt{1-\sin^2(\Omega_E)\sin^2(\Omega_N)}} \qquad \text{(A1_9b)}$$

$$\alpha_N = \frac{-\sin(\Omega_E)\cos(\Omega_N)}{\sqrt{1-\sin^2(\Omega_E)\sin^2(\Omega_N)}} \qquad \text{(A1_9c)}$$

$$\alpha_E = \frac{-\cos(\Omega_E)\sin(\Omega_N)}{\sqrt{1-\sin^2(\Omega_E)\sin^2(\Omega_N)}} \qquad \text{(A1_9d)}$$

In seismology, Ω_E and Ω_N are small. The greatest value of the co-seismic tilts that have ever observed is $4.0\text{x}10^{-4}$ rad (Nigbor, 1994). Thus, we can approximate (A1-9) by:

$$\alpha_P \approx \sin(\Lambda - \Omega_E) \qquad \text{(A1-10a)}$$

$$\alpha_Z \approx 1 \qquad \text{(A1-10b)}$$

$$\alpha_N \approx -\Omega_E \qquad \text{(A1-10c)}$$

$$\alpha_E \approx -\Omega_N \qquad \text{(A1-10d)}$$

Appendix A2: Axis transformations of tilts

Assuming Cartesian coordinate system *NZE* is rotated an angle φ around *Z* to another coordinate system *RZT* (Figure A3). To set up the relationship between components of tilt in these coordinate systems, we start with the coordinate relationship between these two systems:

$$\begin{bmatrix} T \\ R \end{bmatrix} = \begin{bmatrix} \cos(\varphi) & -\sin(\varphi) \\ \sin(\varphi) & \cos(\varphi) \end{bmatrix} \begin{bmatrix} E \\ N \end{bmatrix} \qquad \text{(A2\_1)}$$

or $$T = \cos(\varphi)E - \sin(\varphi)N \qquad \text{(A2\_2a)}$$

$$R = \sin(\varphi)E + \cos(\varphi)N \qquad \text{(A2\_2b)}$$

or $$E = \cos(\varphi)T + \sin(\varphi)R \qquad \text{(A2\_2c)}$$

$$N = \text{-}\sin(\varphi)T + \cos(\varphi)R \qquad \text{(A2\_2d)}$$

Calling U_Z is vertical component of displacement, the components of tilt around *N*, *E*, *R*, and *T* axes, respectively, are defined by (Cochard et al. 2006):

$$\Omega_N = -\frac{\partial U_Z}{\partial E}; \qquad \Omega_E = \frac{\partial U_Z}{\partial N} \qquad \text{(A2\_3)}$$

$$\Omega_R = -\frac{\partial U_Z}{\partial T}; \qquad \Omega_T = \frac{\partial U_Z}{\partial R} \qquad \text{(A2\_4)}$$

Now, using the chain rule leads to:

$$\Omega_R = -\frac{\partial U_Z}{\partial T} = -\left(\frac{\partial U_Z}{\partial N}\frac{\partial N}{\partial T} + \frac{\partial U_Z}{\partial E}\frac{\partial E}{\partial T} \right) \qquad \text{(A2\_5)}$$

$$\Omega_T = \frac{\partial U_Z}{\partial R} = \left(\frac{\partial U_Z}{\partial N}\frac{\partial N}{\partial R} + \frac{\partial U_Z}{\partial E}\frac{\partial E}{\partial R} \right) \qquad \text{(A2\_6)}$$

From (A2_2c) and (A2_2d) we know that:

$$\frac{\partial E}{\partial T} = \cos(\varphi)\,;\ \frac{\partial E}{\partial R} = \sin(\varphi)\,;\ \frac{\partial N}{\partial T} = -\sin(\varphi)\,;\ \frac{\partial N}{\partial R} = \cos(\varphi) \qquad \text{(A2\_7)}$$

Combining (A2_3), (A2_5), (A2_6), and (A2_7) we have the relationship:

$$\Omega_R = \Omega_E \sin(\varphi) - \Omega_N \cos(\varphi) \qquad \text{(A2\_8)}$$

$$\Omega_T = \Omega_E \cos(\varphi) - \Omega_N \sin(\varphi) \qquad \text{(A2\_9)}$$

or

$$\Omega_N = \Omega_R \cos(\varphi) - \Omega_T \sin(\varphi) \qquad \text{(A2\_10)}$$

$$\Omega_E = \Omega_R \sin(\varphi) + \Omega_T \cos(\varphi) \qquad \text{(A2\_11)}$$

Appendix A3: Fundamental formulas

1) Equation of a plane through given three non-linear points $M_1(x_1, y_1, z_1)$, $M_2(x_2, y_2, z_2)$, $M_3(x_3, y_3, z_3)$ can be determined by:

$$\begin{vmatrix} x - x_1 & y - y_1 & z - z_1 \\ x_2 - x_1 & y_2 - y_1 & z_2 - z_1 \\ x_3 - x_1 & y_3 - y_1 & z_3 - z_1 \end{vmatrix} = 0$$

2) The normal unit vector of a plane $Ax + By + Cz + D = 0$ is expressed by:

$$\left\{ \frac{A}{\sqrt{A^2 + B^2 + C^2}}, \frac{B}{\sqrt{A^2 + B^2 + C^2}}, \frac{C}{\sqrt{A^2 + B^2 + C^2}} \right\}$$

3) Cosine of angle between two vectors $\{A_1,B_1,C_1\}$ and $\{A_2,B_2,C_2\}$ can be calculated by:

$$\frac{A_1 A_2 + B_1 B_2 + C_1 C_2}{\sqrt{A_1^{\,2} + B_1^{\,2} + C_1^{\,2}} \sqrt{A_2^{\,2} + B_2^{\,2} + C_2^{\,2}}}$$